Journal of Applied Polymer Science

Cellulose Nanocrystals Extracted from Okra Fibers in PVA Nanocomposites

E. Fortunati,[1] D. Puglia,[1] M. Monti,[1] C. Santulli,[2] M. Maniruzzaman,[3] J. M. Kenny[1,4]

[1]Civil and Environmental Engineering Department, University of Perugia, UdR INSTM Strada di Pentima 4, 05100 Terni, Italy
[2]Sapienza Università di Roma, Chemical Engineering, Materials and Environment Dept., Via Eudossiana 18, 00184, Roma, Italy
[3]Department of Applied Chemistry and Chemical Technology Islamic University, Kushtia 7003, Bangladesh
[4]Instituto de Ciencia y Tecnología de Polímeros, ICTP-CSIC, Juan de la Cierva 3, 28006 Madrid, Spain
Correspondence to: D. Puglia (E-mail: dpuglia@unipg.it)

ABSTRACT: Cellulose nanocrystals (CNC) were extracted from okra bahmia (*Abelmoschus Esculentus*) bast fibers and inserted in different tenors (1, 2, 5, and 10 wt %) as the reinforcement of a poly(vinyl alcohol) (PVA) matrix. The extraction of cellulose was carried out in a two-step procedure: the first chemical treatment led to the production of holocellulose by the gradual removal of lignin, while the subsequent sulphuric acid hydrolysis process allowed obtaining cellulose nanocrystals in an aqueous suspension. The dispersion of CNC in the composite appeared effective at low cellulose content (1 wt %), while it presented more problems for higher contents. However, a 5 wt % cellulose content proved ideal to promote a direct mechanical interaction between the PVA and cellulose structures. Thermal analysis demonstrated that the presence of okra did not have a large effect on glass transition temperature, while it sensibly modified the melting temperature of the PVA matrix, as well as the crystallization temperature, due to the nucleating action of the nanofillers. FTIR spectroscopy performed during the exposure to UV light underlined that no oxidative reactions occur after a short-time exposure and that a longer irradiation times are required to produce oxidation on neat matrix and PVA/CNC nanocomposites. The results confirmed that the presence of CNC does not affect the stability of the neat PVA matrix to the photodegradation after UV irradiation. © 2012 Wiley Periodicals, Inc. J. Appl. Polym. Sci. 000: 000–000, 2012

KEYWORDS: nanoparticles; nanowires and nanocrystals; films; cellulose and other wood products; biomaterials; biopolymers; renewable polymers

Received 26 June 2012; accepted 26 August 2012; published online
DOI: 10.1002/app.38524

INTRODUCTION

Cellulose is one of the most abundant natural biopolymers in the world, which is renewable and biodegradable. Fibrils in nano- and micro-scales generated from cellulose fibers have much higher mechanical properties than those of single fibers. Nanometer-sized single-crystal cellulose, which is commonly referred to as nanocrystalline cellulose, nanowhiskers or nanocrystals (CNC), can be obtained from various sources such as natural fibers and sea animals. The extraction of CNC from renewable sources has gained increasing attention in recent years, because of its exceptional mechanical properties (high specific strength and modulus), large specific surface area, high aspect ratio, environmental benefits, and low cost.[1,2] Extensive studies showed that CNC have great potential application in fields, such as regenerative medicine,[3] optics,[4] and production of composite materials.[5,6] Different approaches have been applied to the preparation of CNC. Each of them leads to different types of nanomaterial, depending on the cellulose raw material composition and its pretreatment, and on the disintegration process. Currently, acid hydrolysis methods are widely used for the removal of amorphous cellulose.[7] CNC can be produced from various resources, such as wood,[1] cotton,[8] ramie,[9] sisal,[10] bacterial cellulose,[11,12] wheat straw,[13] bleached softwood pulps,[14,15] tunicate cellulose,[16] and microcrystalline cellulose (MCC)[17] via the acid hydrolysis method.

Okra bahmia (*Abelmoschus Esculentus*), also known as Lady's finger, is a monocotyledon herbaceous plant of the Malvaceae family, present mainly in the Indian region, but also in the Mediterranean area and in Brazil: from okra's bast, fibers can be extracted, of some use in the food sector, as an added nutrient in gums and pectins. The recent study of their thermal and mechanical behavior indicated okra fibers as a possible candidate for use in the production of biodegradable composites[18] also in view of the maximum length of the extracted fibers, which is in

excess of 60 cm.[19] However, the principal question concerns the possibility to employ these fibers not only as a filler originated from agricultural waste product,[20,21] but ideally to offer some reinforcement to a polymer matrix. If this will prove to be the case, okra bast fiber can play a more significant economical role, adding value to the whole productive system, based on okra bahmia. Okra bast fiber is a lignocellulosic fiber containing a high percentage of α-cellulose. Its composition is around 60–70% α-cellulose, 15–20% hemicellulose, 5–10% lignin, and 3–5% pectins, together with some water soluble matter.[22] However, such it is the case for other fibers from herbaceous plants, the use of okra bast fibers in textiles present a number of drawbacks i.e., limited rub resistance, scarce color fastness, sensitivity to wear and it is very much prone to creasing, possibly because of high degree of orientation of cellulose in the fiber. Moreover, previous studies did not appear nonetheless to demonstrate that most common chemical treatments, such as bleaching or alkalization, substantially improve the fiber properties, so that in the end the variability of their mechanical properties would remain far too high also for their possible use in composites.[23,24] This suggests that the use of okra fibers as the source of CNC may be a viable alternative to employing them in the form of technical fibers.

Poly(vinyl alcohol) (PVA) has been extensively investigated as a controlled drug release hydrogel, a membrane material for chemical separations, barrier membrane for food packaging, pharmaceutical component, manufacturing material for artificial human organs, and as a biomaterial.[25–27] The incorporation of functional materials into PVA matrix has been studied with the general aims of either providing reinforcement for artificial tissue applications[28] or enhancing drug delivery.[29] Moreover, many researchers dispersed reinforcement structures as cellulose fibers in the hydrophilic polymers of poly(vinyl alcohol) to study their reinforcement effects.[30,31] Mechanical tests have shown a strong reinforcement effect.[32]

In this work, we used okra natural fiber, as extracted from its bast, as the source material to produce cellulose micro- and nano-fibers, with a view to obtaining cellulose structures with a high crystallinity and thermal stability, by means a pretreatment with alkali, followed by sulphuric acid extraction. The main objectives of this study is to produce new biopolymer nanocomposites with good mechanical properties, thermal stability, maintaining the optical transparency of the selected PVA matrix, and at the same time to develop an energy efficient and friendly environmental processing methodology. The possibility of using these materials in packaging applications suggested the need of investigating their stability under UV exposure.

EXPERIMENTAL

Materials

Poly(vinyl alcohol) (PVA) supplied by Sigma Aldrich (USA) (31,000–50,000 g/mol, 87–89% hydrolyzed) was used as matrix for the nanocomposite preparation.

Okra, whose local name is Dherosh, has been collected in Kushtia District (Bangladesh). After collection, the fresh plant was kept under water to allow microbial degradation, a process known as water retting, which is based on the fact that microbes attack preferentially the nonstructural bonding components, such as pectin, allowing to more easily separate the single technical fibers from the stem. Within 15–20 days, the stems degraded sufficiently to enable fiber extraction. The fibers were isolated from the degraded stems by being washed three times using deionized water. In this way, it can be considered that most part of the fibers present in the fresh plant can be extracted, the only losses being linked to the fact that only the middle part of the stem, corresponding to about 50–70% of the length of the plant, is used for this purpose.

The fibers obtained at this point are referred hereinafter to as "pristine okra fibers": these were then tied with ropes, dried in open air and kept in moisture-proof container afterwards. To analyze their cross-section, okra fibers were cut by hand and mounted into an epoxy-based compound, then polished to achieve a flat surface.

Okra Fiber Pretreatment

To obtain therefore pure crystalline fractions from the pretreatment of the selected natural fiber, okra fibers were first washed with distilled water several times, dried, and chopped to an approximate length of 5–10 mm. Subsequently, a dewaxing step was carried out by boiling the fibers in a toluene/ethanol mixture (2:1 volume/volume) for 6 h. This was followed by filtering, washing with ethanol for 30 min, and drying in an oven. Finally, an alkali treatment procedure was selected for cellulose extraction. Okra fibers were first treated with 0.7 wt/vol % of sodium chlorite $NaClO_2$; the fibers (liquor ratio 1:50) were boiled for 2 h and the solution pH was lowered to about 4 by means of acetic acid for the bleaching. A treatment with sodium bisulphate solution at 5 wt/vol % was carried out and at the end of this preliminary chemical process, holocellulose (α-cellulose + hemicellulose) was obtained, by the gradual removal of lignin.[33] The holocellulose was treated with 17.5 wt/vol, % NaOH solution, filtered and washed with distilled water. The obtained cellulose was dried at 60°C in a vacuum oven until constant weight.

Cellulose Nanocrystal Production

Cellulose nanocrystal (CNC) suspension was prepared from okra treated fibers by sulphuric acid hydrolysis following the recipe used by Cranston and Gray.[34] Hydrolysis was carried out with 64 wt/wt % sulphuric acid at 45°C for 30 min with vigorous stirring. This reaction time was selected to guarantee the reaction efficiency and avoid the fiber degradation. Immediately following the acid hydrolysis, the suspension was diluted 20-fold with deionized water to quench the reaction. The suspension was centrifuged at 4500 rpm for 20 min to concentrate the cellulose crystals and to remove excess aqueous acid. The resultant precipitate was rinsed, recentrifuged, and dialyzed against deionized water for 5 days until constant neutral pH was achieved. The suspension was sonicated repeatedly (Vibracell 75043, 750 W, Bioblock Scientific, USA) at 30% output (while cooling in an ice bath) to create cellulose crystals of colloidal dimensions. The final yield after the hydrolysis process was calculated as % (of initial weight) of the used pretreated okra fibers.

Treated Okra Characterization Methods

The microstructure and agglomeration effects of cellulose structures obtained after the pretreatment process and the morphology and size of cellulose nanocrystals produced during the acid hydrolysis were investigated by means of field emission scanning electron microscope (FESEM, Supra 25-Zeiss, Germany).

The pretreated cellulose was swollen in distilled water before FESEM observation. A 1 wt % aqueous solution of cellulose was stirred for 4 h at room temperature. The solution was then subjected to 0.5 h sonication over 4 h in 10 min intervals, in order to loosen up the cellulose particles. Few drops of the suspension were cast onto silicon substrate, vacuum dried for 2 h and gold sputtered before the analysis.

The FESEM micrographs of the pretreated cellulose fibers were also analyzed with the NIS-Elements BR (Nikon, USA) software in order to determine the fiber diameter after the pretreatment. Sixty measurements were performed and subsequently plotted in a histogram to offer a visual impression of diameter distribution.

Cellulose nanocrystal suspension after the acid hydrolysis was directly cast on to silicon and observed by FESEM after the gold sputtering.

Thermogravimetric measurements (TGA) of 10 mg of pristine okra fiber, pretreated okra, and dried cellulose nanocrystals were performed by using a Seiko Exstar 6300, UK analyzer, to evaluate the effect of both pretreatment and acid hydrolysis on the thermal behavior of okra fibers. Heating scans from 30 to 900°C at 10°C/min in nitrogen atmosphere were performed for each sample.

PVA Nanocomposite Based on Cellulose Nanocrystal

Poly(vinyl alcohol) (PVA) nanocomposite films reinforced with cellulose nanocrystals (CNC) were prepared by solvent casting in water. PVA aqueous solutions were firstly prepared. Depending on the desired nanocrystal proportion in PVA matrix, a given amount of PVA (1.5 g) was dissolved in 15 ml distilled water at 80°C for 2 h under mechanical stirring. Then, the solutions were kept under stirring to reach room temperature (RT). To obtain films with different compositions, the solutions were mixed with a specific amount of the aqueous dispersion of cellulose nanocrystals and sonicated (Vibracell 75043, 750 W, Bioblock Scientific, USA) for 2 min. The resulting mixture was cast onto a glass Petri dish and placed in a 37°C oven to evaporate water. Cellulose nanocrystal content in the final nanocomposites were 0, 1, 2, 5, and 10 wt % respect to the polymer weight and the samples were designed PVA, PVA/1CNC, PVA/2CNC, PVA/5CNC, and PVA/10CNC, respectively. The obtained films were 100–200 μm thick.

Nanocomposite Characterization

The transparency of PVA nanocomposite systems was evaluated by absorption measurements. A Perkin Elmer Instruments (Lambda 35, USA) UV-Vis spectrophotometer, working in the wavelength between 250 and 900 nm, was used in order to investigate the optical properties of the produced composites. Fourier infrared (FTIR) spectra of neat PVA and PVA/CNC nanocomposites were also recorded using a Jasco FTIR 615, USA spectrometer in the 400–4000 cm^{-1} range, in attenuated reflection mode (ATR). The optical properties of the materials were also recorded both at time 0 and after 144 h of UV exposure; specifically, FTIR measurements were taken within intervals of 48 h for all the materials after the exposure to UV lamps at a wavelength of 366 nm (TRIWOOD lamp 6/36).

The mechanical behavior of neat PVA and PVA/CNC nanocomposite systems was evaluated by tensile tests, performed, as prescribed by UNI ISO 527, on rectangular samples (100 × 10 mm^2). The test was carried out by means of a digital Lloyd Instrument LR 30 K, UK, and the initial grip separation was 50 mm long. Load was measured by using a 500 N cell, and applied in displacement control with a crosshead speed of 5 mm/min. Elongation at break (ε_b), and Young's modulus (E) were considered and calculated from the resulting stress–strain curves. The measurements were performed at RT and at least five samples for each formulation were tested.

The microstructure of PVA nanocomposite films was investigated using a scanning electron microscope, FESEM, Supra 25-Zeiss, Germany. Cryo-cross sections of the nanocomposites were sputtered with gold and then analyzed.

Differential scanning calorimeter (DSC, Mettler Toledo 822/e, USA) measurements were carried out in the temperature range from −25 to 220°C, at 10°C/min, performing two heating and one cooling scan.

The glass transition temperature (T_g) was taken as the inflection point of the specific heat increment at the glass–rubber transition while the melting temperature (T_m) and the crystallization temperature (T_c) was taken as the peak temperature of the endothermic and exothermic heat profiles, respectively. Five milligrams of each sample were tested, while for each formulation three specimens were used.

The crystallinity degree was calculated as:

$$\chi = \frac{1}{(1 - m_f)} \left[\frac{\Delta H}{\Delta H_0} \right] * 100 \qquad (1)$$

where ΔH, is the enthalpy for melting or crystallization, ΔH_0 is enthalpy for melting of a 100% crystalline PVA sample, taken as 161.6 J/g[35] and (1-m_f) is the weight fraction of PVA in the sample.[36]

RESULTS AND DISCUSSION

Morphological Characterization of Treated Cellulose

The original structure of the unmodified okra fibers used as starting material is shown in Figure 1(Aa, Ab), and it can be seen that the fiber dimensions are in the order of 90 μm. Figure 1A(c–d) show FESEM observations at different magnifications of the okra fibers obtained after the chemical treatment. The fibers appear separated into individual micro-sized structures. Figures 1(Ac, Ad) show well-organized networks of cellulose microfibers where individual microfibers with compact structure can be recognized. The pretreatment process has moderately split the fibers and increased their surface area. According to the literature, a number of surface treatments can be applied on

Applied Polymer SCIENCE

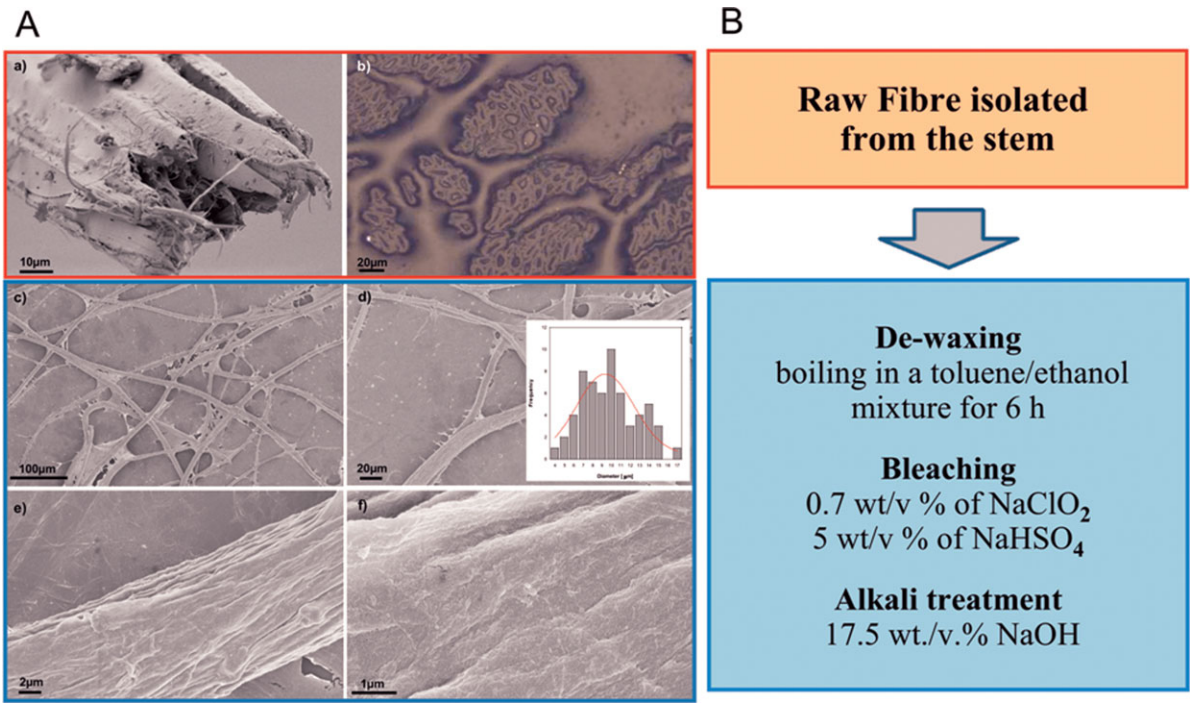

Figure 1. A. Morphological characterization of fractured pristine okra fiber (a, b), and FESEM observation of chemical pretreated okra at different magnifications (c–f). The insert shows the diameter distribution of the pretreated okra fibers. B: Scheme of the okra fiber pretreatment. [Color figure can be viewed in the online issue, which is available at wileyonlinelibrary.com.]

plant fibers[37] to obtain the technical fiber. Some of them, such as alkali-treatment e.g., with sodium hydroxide (NaOH), bleaching with sodium hypochlorite (NaClO) or chlorite ($NaClO_2$), are usually applied on the fiber bundles, with the aim of exposing as much as possible the cellulose structure, increasing the number of reaction sites.[38] This result can be achieved by removing as much as possible nonstructural matter i.e., hemicellulose, lignin, and pectin.[39] Our previous results confirm that modifications caused to okra fiber surface by the most divulgated chemical treatments (scouring, bleaching with 10% sodium chlorite and bleaching with 10% sodium chlorite followed by 1% sodium hydroxide alkalization) generally decreased the thermal stability and the mechanical properties of the fiber.[23] However, these chemical treatments are useful and suitable for removing amorphous fractions in the raw fibrous material and reduced the diameter of the fiber. Figure 1(B) briefly summarizes the chemical treatment phases. After the chemical treatment most of the lignin and hemicellulose were removed. The chemical procedures conduct to the partial removal of these fibers components, yielding a diameter reduction (by separating the macro into micro fibrils) as well as a change in the fiber composition (cellulose purification). The diameters of the cellulose fibers obtained after the chemical pretreatment were analyzed with the NIS-Elements BR (Nikon) software on the basis of FESEM investigation. A histogram of the diameter distribution of the okra fibers, characterized by an average diameter of 9.8 μm, is included as an insert in Figure 1(A). This evaluation underlined the effect of applied chemical treatment on cellulose fiber morphology and size. FESEM micrographs at higher magnification [Figure 1A(e, f)] show that the bleaching procedure resulted in the partial defibrillation of fiber as the consequence of the elimination of cementing component. Moreover, each microfiber can be considered as a bundle of cellulose nanostructures, linked along the microfibril by amorphous domains. The FESEM image of the hydrolyzed material validates the effectiveness of the acid treatment [Figure 2(a)]. Moreover, a photograph of CNC suspension is shown in Figure 2(b). The transparency of CNC-based solution indicates that the dimensions of a major part of cellulose particles in the suspension are below the limit for light scattering confirming the FESEM analysis and highlighting the success of the hydrolysis process. The morphological investigation indeed confirms the predominant presence, in the aqueous suspensions, of needle-like cellulose nanocrystals and the existence of a significant number of crystal aggregates, whose presence is likely to be due to a time limited process. The selection of hydrolysis parameters was done considering our previous experimental approach on MCC,[40] but selected parameters, as time and temperature, should be probably re-discussed and further investigated in the case of hydrolysis starting from a macrofiber instead of a microcrystalline material. The presence of aggregates might be certainly due to the short reaction time adopted, and the aggregates can be eliminated extending the reaction times, but careful investigation should be considered in this case, taking into account that a prolonged hydrolysis reaction could degrade the vegetable tissue of this herbaceous bast fiber. However, a good hydrolysis yield of about 30%, close to the value estimated for an optimized hydrolysis, was obtained, highlighting the effectiveness of the two-step process followed.

Figure 2. (a) FESEM micrograph of okra cellulose nanocrystals obtained by acid hydrolysis and (b) image of CNC solution.

Thermal Characterization of Treated Cellulose

Thermogravimetric (TG) and derivative thermogravimetric (DTG) curves of untreated okra, pure cellulose derived from okra (after removal of lignin and hemicellulose) and the acid hydrolyzed cellulose from okra (i.e., cellulose nanocrystals) are shown in Figure 3. According to other studies on lignocellulosic fibers[41,42] the TG curve of okra fiber [Figure 3(a)] shows three weight loss steps, while its decomposition occurs in two main stages. The initial weight loss is attributed to vaporization of water from the fibers, while the onset of degradation for the okra fibers occurs at higher temperature, precisely after 220°C. Above this temperature it can be seen that the thermal stability is gradually decreasing [Figure 3(b)] and the degradation of the okra fibers proceeds. In particular, the first stage is associated to the thermal depolymerization of hemicellulose and pectin and to the cleavage of glycosidic linkages of cellulose, while the second one corresponds to the degradation of α-cellulose present in the fiber. As expected in the case of alkali treated fiber, the main peak, attributed to the decomposition of hemicellulose disappeared, while in the case of CNC, a small broadening or shoulder on the left side of the main peak appears. This peak was attributed to the broad distribution of molecular mass from cellulose or to a residual presence of hemicellulose.[12,43]

Cellulose Nanocrystal and PVA-Based Nanocomposites: Transparency and Morphological Properties. Figure 4 shows UV-Vis characterization and photos (insert) of PVA and PVA/CNC nanocomposite films. Through casting from an aqueous solution, the PVA film control gave a transparent and flexible film (data not shown). The PVA/cellulose nanocrystal nanocomposites still showed flexibility while maintaining the optical transparency of the polymer matrix, even if the yellowing effect (due also to the initial color of the CNC aqueous solution) was more evident with increasing CNC content. The transparent

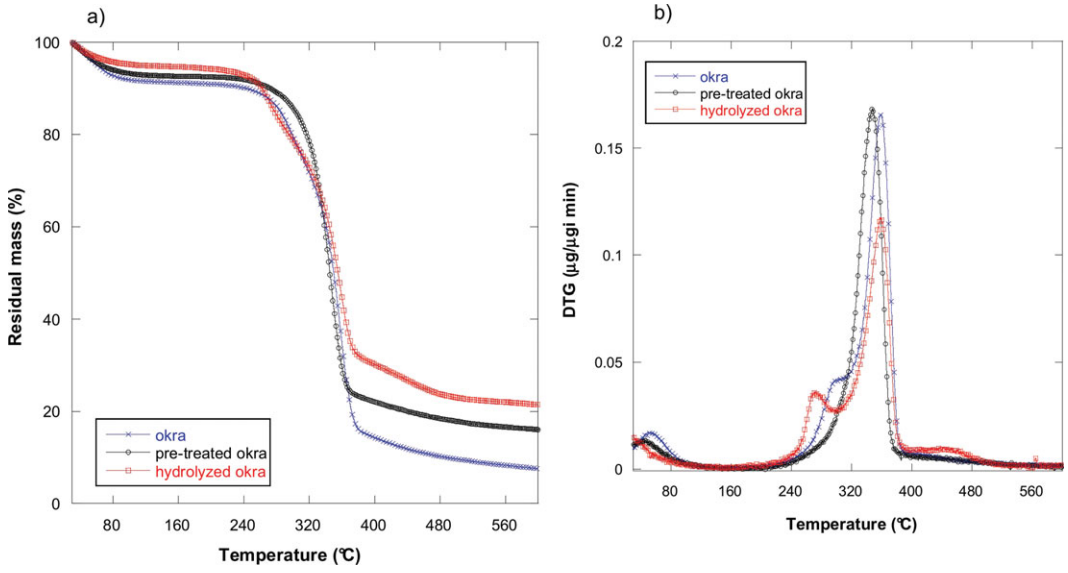

Figure 3. TG (a) and DTG (b) curves of untreated, pretreated, and hydrolyzed okra fiber. [Color figure can be viewed in the online issue, which is available at wileyonlinelibrary.com.]

Applied Polymer SCIENCE

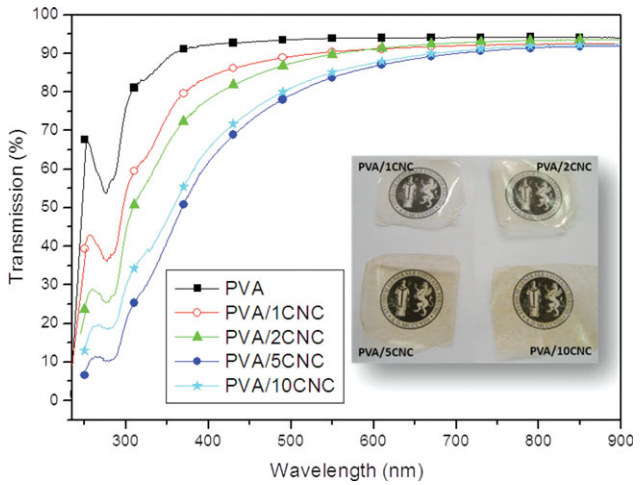

Figure 4. UV-Vis spectra and visual observation (insert) of PVA and PVA/CNC nanocomposites. [Color figure can be viewed in the online issue, which is available at wileyonlinelibrary.com.]

nature of these nanocomposites is a result of the largest dimension of CNC being far smaller than the wavelength of visible light.

The transmission spectra of PVA film and PVA nanocomposite systems with different amount of CNC were investigated. PVA film shows a very low transmission intensity (10%) at 250 nm, a sharp increase in the transmission intensity reaches 93% at 450 nm and then the transmission intensity is approximately constant at this value in the wavelength range 500–900 nm. PVA film practically does not absorb above 250 nm, which is obvious because of the very high hydrolysis degree of the rough polymer. Abd El Kader[44] reported that PVA samples in UV region, show two absorption bands at 284 and 327 nm, related to high energy absorption assigned as π-π^* bonds (mainly C=O and/or C=C), which are present in the tail head of the polymer, and influenced by its molecular weight. The presence of cellulose in PVA matrix reduces the transmission capability of the polymer and this effect is influenced by the CNC content. PVA/CNC nancomposites show a slower transmission increase in the wavelength range between 300 and 450 nm respect to PVA film, and reach 85 and 80% for PVA/1CNC and PVA/2CNC and about 70% for both PVA/5CNC and PVA/10CNC at 450 nm. Moreover, starting from 650 nm, all nanocomposite formulations keep a constant transmission level of about 92%. The reduction in transmission level between 300 and 450 nm for nanocomposite formulations is influenced by volume fraction of the nanoreinforcement that can have a large influence on the transmittance of UV and visual light and it is influenced by the CNC content that is also able to modify the sample color (Figure 4, insert). However, the reduction in transmission of UV and visual radiation through the material is an advantage when using PVA nanocomposites in packaging applications, since UV and visible light can have a negative effect on the quality of packed food.

Field emission scanning electron microscopy of PVA and PVA/CNC nanocomposite fracture surfaces were performed to evaluate sample morphology and to analyze cellulose dispersion in the PVA matrix (Figure 5).

FESEM images of fractured surfaces showed a smooth surface for PVA matrix [Figure 5(a, b)]. A rough texture with small cracks was observed in the presence of 1 wt % of CNC [Figure 5(c, d)]. The fracture initiated crack formation, but well-dispersed CNC and good bonding between the components evidently prevented further crack proliferation. The rough texture could be attributed to the addition of cellulose nanocrystals, which added to the stiffness and brittleness of the films. Nanocomposites with higher content of cellulose [i.e., 10 wt % in Figure 5(e, f)] underlined more cracks and a more evident roughness in the fracture surfaces. Moreover, in PVA/10CNC sample, white small dots appeared in the analyzed cross-section. This may indicated that there is very limited cellulose aggregation in PVA, evident only in the formulation with the highest content of CNC, as the result of the high level of compatibility and interaction between the hydrophilic crystalline nanocellulose and PVA matrix.[45]

Thermal Analysis. TGA analysis was performed in a nitrogen atmosphere, in order to study the thermal stability of the produced materials. The presence of three degradation steps for the produced films is evident from derivative thermogravimetric curves (DTG) of the weight loss profiles (Figure 6). All the samples showed a similar initial weight loss resulting from the loss of moisture in PVA upon heating. After moisture desorption, two main decomposition stages were observed in the DTG curve for the neat PVA film and okra CNC-based nanocomposites. The second and third degradation steps were consistent with the generally accepted mechanism for the degradation of PVA.[46,47] The peak temperature related to the second step of decomposition for the neat matrix was similar for the PVA/CNC nanocomposites and PVA film, while the maximum degradation rate was reduced with the addition of CNC to the PVA matrix up to a 5 wt % content, such as a lower onset decomposition temperature for the nanocomposites was detected. This weight loss is consistent with the presence of CNC and corresponded to the pyrolysis of cellulose crystals catalyzed by acid sulphate groups. This decrease is clearly visible in the case of PVA/10CNC, in which the thermal stability of the system is slightly compromised, with a reduction of the main degradation temperature of the PVA of about 30°C. This behavior is clearly due to the increasing amount of crystalline material since, as observed before in the TGA analysis of CNC, a shoulder on the left side of the main peak was observed due to the early thermal degradation of the crystals.[45–47]

The thermal properties of CNC based nanocomposites were also studied from DSC thermograms. The glass transition temperature, crystallization, and melting temperatures of unfilled polymer matrix and nanocomposite films reinforced with CNC from okra up to 10 wt %, such as the crystallinity value for second heating scan, were measured and reported in Table I. Regardless the composition, T_g of PVA remains roughly constant when adding okra cellulose nanocrystals. Only a slight increase can be noted in the case of PVA/5CNC and PVA/10CNC. This behavior can be explained by the small size of the

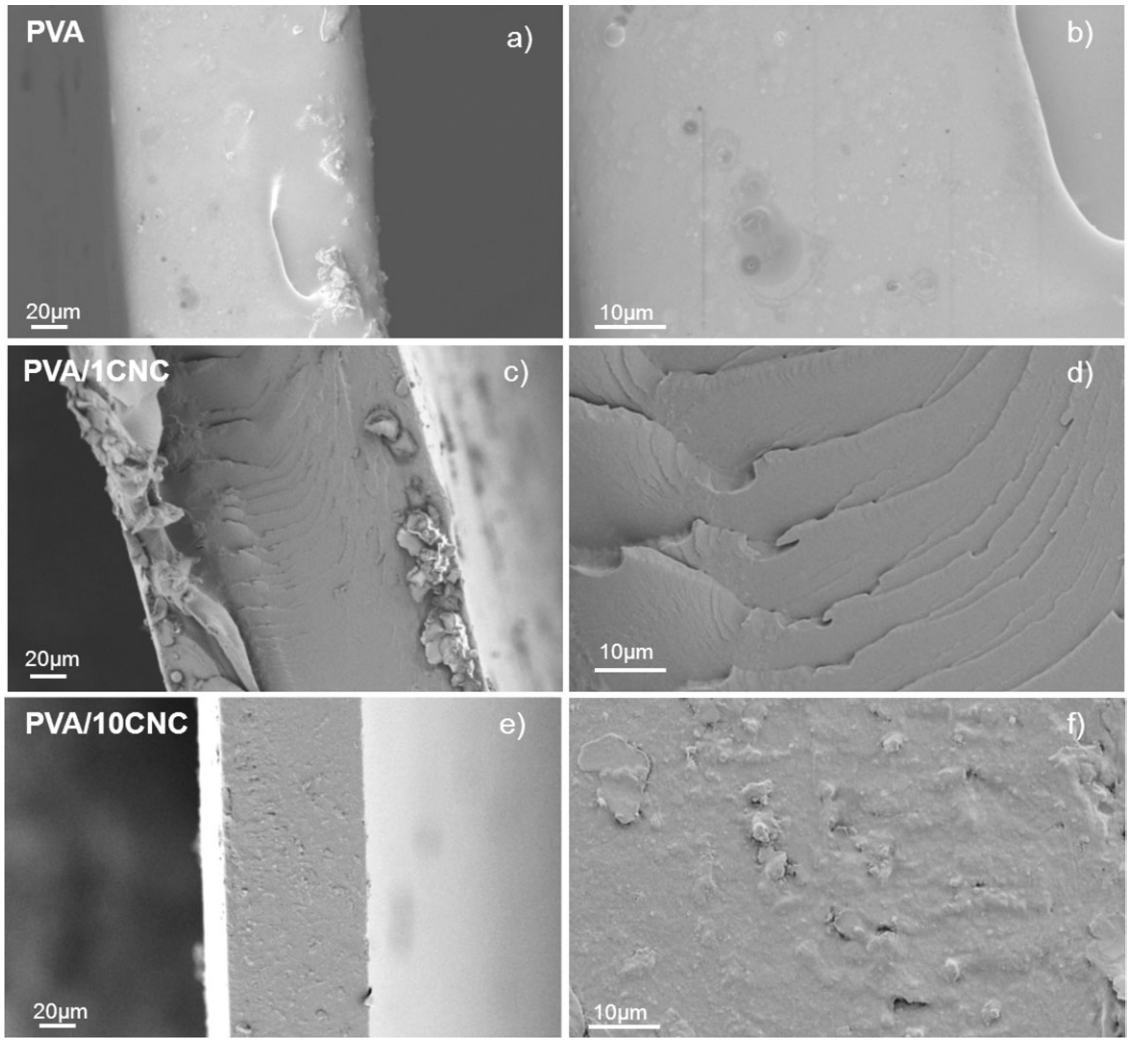

Figure 5. FESEM images of fractured surfaces of neat PVA (a, b) and PVA/1CNC (c, d), PVA/10CNC (e, f) nanocomposites.

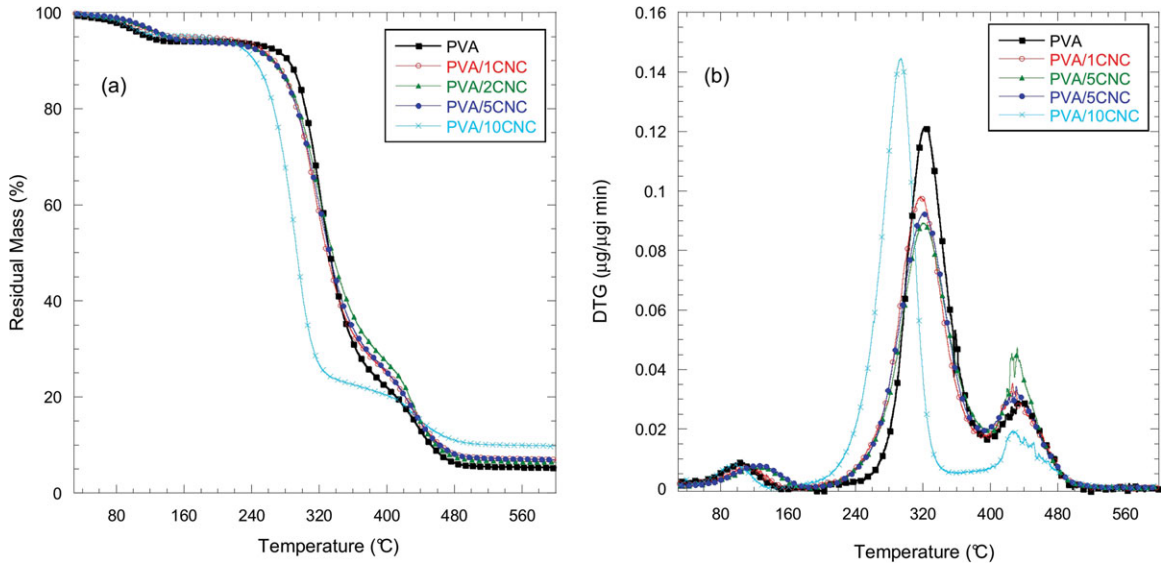

Figure 6. TG (a) and DTG profiles (b) for neat PVA and PVA/CNC nanocomposites in nitrogen atmosphere. [Color figure can be viewed in the online issue, which is available at wileyonlinelibrary.com.]

Table I. Thermal Properties of PVA and PVA/CNC Nanocomposites at the Second Heating Scan

	Second heating scan			
Samples	T_g (°C)	ΔH_m (J/g)	T_m (°C)	X_c (%)
PVA	69.0 ± 0.1	19.8 ± 2.3	176.7 ± 2.7	12.2 ± 1.0
PVA/1CNC	68.7 ± 0.2	27.1 ± 1.8	184.5 ± 0.1	17.0 ± 1.0
PVA/2CNC	69.0 ± 0.4	22.6 ± 0.9	182.3 ± 2.0	14.3 ± 0.6
PVA/5CNC	70.1 ± 0.9	26.1 ± 0.5	179.5 ± 0.1	17.1 ± 0.3
PVA/10CNC	69.0 ± 0.1	29.1 ± 3.0	188.0 ± 0.7	20.0 ± 2.0

The crystallinity degree was calculated according to eq. (1).

crystals, which did not cause massive breaks of hydrogen bonds in PVA. Nevertheless, it seems that the interactions were not strong enough to slow the chain mobility associated with glass transition, since the T_g values measured on PVA nanocomposites samples were close to that of neat PVA. A detectable increase of crystallinity was measured for all the nanocomposite systems in the second heating scan, due to a nucleating effect of the nanosized CNC.[48]

Mechanical Behavior. The mechanical behavior of conditioned neat PVA and PVA/CNC nanocomposites was evaluated and tensile test results are reported in Figure 7. The histograms show the elongation at break [Figure 7(a)] and Young's modulus values [Figure 7(b)] for different systems. A decrease of the elongation at break of 86% for PVA/1CNC and 57% for PVA/2CNC systems with respect to PVA neat matrix, was revealed. The reduced elongation at break with the addition of fibers in the polymer, is a common trend observed in thermoplastic composites, in which the addition of stiff reinforcements causes stress concentrations.[49] However, a large increase in the elongation at break value was detected for PVA/5CNC sample that shows ca. 130% deformation respect to 50% of the polymer matrix, while the PVA/10CNC shows the lowest value of strain underlining the brittleness of the system due to the high content of cellulose. The elongation at break is affected by the volume fraction of the added reinforcement, the dispersion in the matrix, and the interaction between the reinforcement and the matrix.[49] In our case, cellulose nanocrystals at 1 or 2 wt % showed a reduced ultimate strain as the consequence of local stress concentrations, while 5 wt % content is ideal to promote a direct interaction between the PVA and cellulose structures. This is of great importance since it leads the available surface area of cellulose to its optimal dimension, as previously reported.[50]

Figure 7(b) compares the modulus of PVA matrix and PVA/CNC nanocomposite films. PVA film showed a Young's modulus of 1.3 GPa while a reduction of 46% was observed for PVA/1CNC system. Comparable values of Young's modulus were measured for PVA/2CNC and PVA/5CNC respect to the polymer matrix and PVA/10CNC showed the highest value of the elastic modulus (1.9 GPa) confirming also the value of elongation at break, which is reported in Figure 7(a). The results obtained for nanocomposite mechanical behavior in the elastic and plastic region are critical for their employment in the industrial application field where a high elongation at break combined to an increment in tear resistance are required. In our case, a 5 wt % of cellulose nanocrystals in PVA matrix does not modify the mechanical behavior in the elastic region, while it improves the plastic response of the systems.

FTIR Characterization after UV Exposure. FTIR spectra (wavenumbers range between 3600 and 600 cm^{-1}) of pure PVA and PVA/CNC nanocomposites before UV weathering are

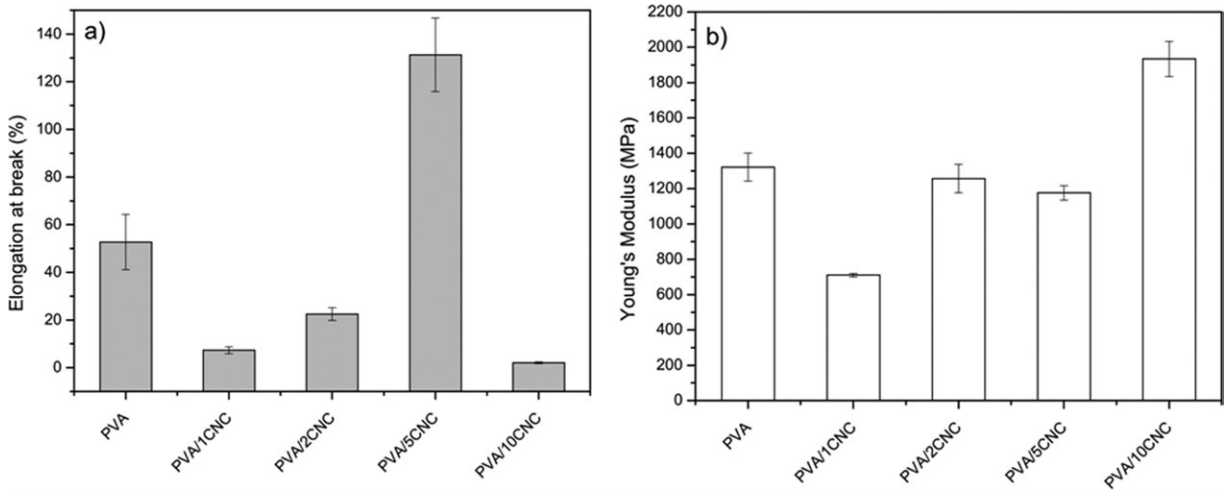

Figure 7. Elongation at break (a) and Young's Modulus values (b) for PVA and PVA/CNC nanocomposites.

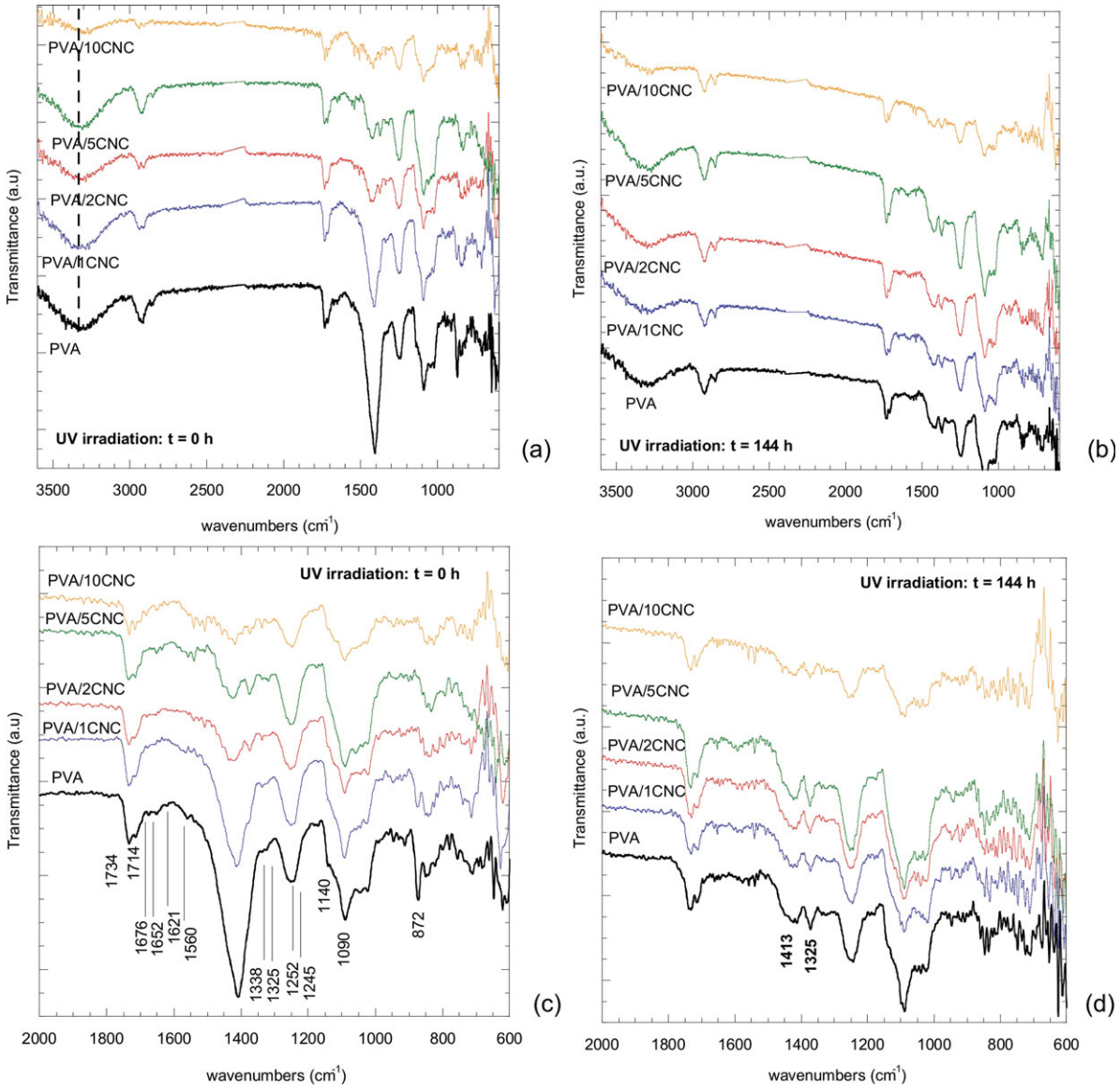

Figure 8. FTIR analysis in the 3600–600 cm^{-1} range of neat PVA and PVA/CNC nanocomposites at initial time (a) and after 144 h (b) of UV irradiation; zoom of the FTIR spectra in the range 2000–600 cm^{-1} for PVA and PVA/CNC composites before (c) and after irradiation (d).[Color figure can be viewed in the online issue, which is available at wileyonlinelibrary.com.]

reported in Figure 8(a), while the infrared spectra of the same materials after short time UV exposure (144 h) are reported in Figure 8(b). IR spectrum of neat PVA [Figure 8(a)] exhibits several bands characteristic of stretching and bending vibrations of O—H, C—H, C=C, and C—O groups. A broad band observed from 3200 to 3550 cm^{-1} in the PVA spectra corresponding to the hydroxyls (—OH) stretching due to the strong hydrogen bond of intramolecular and intermolecular type, which indicate the presence of hydroxyl groups. In this specific range, the addition of okra CNCs to the PVA matrix has only a slight effect on the intensity of OH stretching, while it can be observed that, compared to CNC-free matrix, PVA nanocomposites with increased amounts of CNC yielded a shift of the main OH peak region to lower wavenumbers (from 3322 cm^{-1} for neat PVA to 3285 cm^{-1} for PVA/10CNC). This can be explained by the hydrogen bonding interactions between the hydrophilic CNC particles and PVA medium (—OH groups on the surface of nanocrystals interacting with adjacent —OH groups in the PVA). Observing the spectra in the range 2000–600 cm^{-1} [Figure 8(c)], the bands observed at 1734 and 1652 cm^{-1} are indeed considered to be due to acetate C=O and C=C stretching modes, respectively, while the band observed at 1375 cm^{-1} is attributed to the C—H bending mode. The strong band at 1245 cm^{-1} is assigned to the ester acetate C—O bending mode and other peaks located at 1413 cm^{-1}, assigned to the symmetric (*vs.*) stretching vibration of the —COO— group, and 1092 cm^{-1}, due to C—O stretching can be found related to PVA.[51,52] The cluster of absorptions at 1375, 1325, and 1252 cm^{-1} can be attributed to the bending of CH, CH_2, and OH of okra CNCs, which are typical characteristics of polysaccharide

components.[53,54] The intensity of the broad band peak in the region of 1413 cm^{-1} decreases with the addition of okra CNC to the PVA matrix, while the intensity of the peak at 1325 cm^{-1} due to the cellulose component increases when compared to the peak at 1413 cm^{-1} after UV exposure [Figure 8(d)]. This indicates that the contribution of C—O stretching from the cellulosic component is becoming more significant with the increasing amount of okra. After UV weathering, a decrease in the O—H stretching vibration peak was also observed when compared to pure PVA. This result suggests that the hydrogen bonding becomes weaker in PVA/CNC nanocomposites than in pure PVA, due to the diminution in the number of OH groups. No oxidative reactions were detected after the short-time exposure, since longer irradiation times are required to produce oxidation on neat matrix and PVA/CNC nanocomposites. The results confirmed that the presence of CNC does not affect the stability of the neat PVA matrix to the photodegradation after UV irradiation.

CONCLUSIONS

The extraction of cellulose nanocrystals (CNC) from okra bahmia bast fibers has been considered, to produce PVA based nanocomposites with maximum cellulose content of 10 wt %, with the objective of studying its compatibility with the polymer matrix and the possible reinforcement effect on the nanocomposite. The hydrolysis parameters applied, though building on previous investigations of extraction starting from microcrystalline material, proved also sufficiently suitable for hydrolysis from a macrofiber, such as okra. Further improvements could possibly be obtained by increasing the reaction times, though it would also need to be verified whether this is compatible with not inducing an excessive degradation of the herbaceous fiber.

The very limited cellulose aggregation encountered in PVA, which is evident only in the formulation with the highest content of CNC, appears to demonstrate the good level of compatibility between the hydrophilic crystalline nanocellulose and the polymer matrix. Cellulose nanocrystals are able to increase the crystallinity degree of PVA matrix and the nanocomposites containing 5 wt % of cellulose appeared the ideal formulation suggesting that this content may lead the available surface area of cellulose to its optimal dimension in the nanocomposite. The obtained results showed some potential for okra fibers, and in general for bast herbaceous fibers, for their application in the form of CNC in nanocomposite systems. In particular, they indicated some possibility, via a thorough control of the hydrolysis process, to overcome some of the inherent limits (large geometrical variability, limited resistance to chemical treatment), previously revealed when considering the possible use of okra macrofibers as filler for polymer matrices.

REFERENCES

1. Habibi, Y.; Lucia, L. A.; Rojas, O. *J. Chem. Rev.* **2010,** *110*, 3479.
2. Lima, M. M. D. S.; Borsali, R. *Macromol. Rapid Commun.* **2004,** *25*, 771.
3. Fleming, K.; Gray, D. G.; Matthews S. *Chem. Eur. J.* **2001, 7, 1831.**
4. Iwamoto, S.; Nakagaito, A. N.; Yano, H.; Nogi, M. *Appl. Phys. A* **2005,** *81*, 1109.
5. Ruiz, M. M.; Cavaille, J. Y.; Dufresne, A.; Graillat, C.; Gerard, J. F. *Macromol. Symp.* **2001,** *169*, 211.
6. Bhatnagar, A.; Sain, M. J. *J. Reinforced Plast. Compos.* **2005,** *24*, 1259.
7. Revol, J. F.; Bradford, H.; Giasson, J.; Marchessault, R. H.; Gray, D. G. *Int. J. Biol. Macromol.* **1992,** *14*, 170.
8. Dong, X. M.; Revol J. F., Gray D. G. *Cellulose* **1998,** *5*, 19.
9. De Menezes, A. Jr.; Siqueira, G.; Curvelo, A. A. S.; Dufresne, A. *Polymer* **2009,** *50*, 4552.
10. Moran, J. I.; Alvarez, V. A.; Cyras, V. P.; Vazquez, A. *Cellulose* **2008,** *15*, 149.
11. Araki, J.; Kuga, S. *Langmuir* **2011,** *17*, 4493.
12. Roman, M.; Winter, W. T. *Biomacromolecules* **2004,** *5*, 1671.
13. Helbert, W.; Cavaille, J. Y.; Dufresne, A. *Polym. Compos.* **1996,** *17*, 604.
14. Araki, J.; Wada, M.; Kuga, S.; Okano, T. *J. Wood Sci.* **1999,** *45*, 258.
15. Beck-Candanedo, S.; Roman, M.; Gray, D. G. *Biomacromolecules* **2005,** *6*, 1048.
16. Favier, V.; Chanzy, H.; Cavaille, J. Y. *Macromolecules* **1995,** *28*, 6365.
17. Bondeson, D.; Mathew, A.; Oksman, K. *Cellulose*, **2006,** *3*, 171.
18. De Rosa, I. M.; Kenny, J. M.; Puglia, D.; Santulli, C.; Sarasini, F. *Compos. Sci. Technol.* **2010,** *70*, 116.
19. Srinivasa Babu, N.; Murali Mohan Rao, K.; Suresh Kumar, J. *Int. J. Eng.* **2009,** *3*, 403.
20. Pakzad, A.; Simonsen, J.; Yassar, R. *Compos. Sci. Technol.* **2012,** *72*, 2, 314.
21. Benchasri, S. *Ratar. Povrt.* **2012,** *49*, 105.
22. Jarret, R. L.; Wang, M. L.; Levy, I. J. *J. Agric. Food Chem.* **2011,** *59*, 4019.
23. Moniruzzaman, M. D.; Maniruzzaman, Mohd.; Gafur, Ma.; Santulli, C. *J. Biobased Mater. Bioenergy* **2009,** *3*, 286.
24. De Rosa, I. M.; Kenny, J. M.; Maniruzzaman, M.; Moniruzzaman, M.; Monti, M.; Puglia, D.; Santulli, C.; Sarasini, F. *Compos. Sci. Technol.* **2011,** *71*, 246.
25. Lange, J.; Wyser, Y. *Packaging Technol. Sci.* **2003,** *16*, 149.
26. Schmedlen, R.; Masters, K.; West, J. *Biomaterials* **2002,** *23*, 4325.
27. Wan, W.; Campbell, G.; Zhang, Z.; Hui, A.; Boughner, D. *J. Biomed. Mater. Res.* **2012,** *63*, 854.
28. Wan, W. K.; Hutter, J. L.; Millon, L.; Guhados, G. In Cellulose Nanocomposites: Processing, Characterization and Properties; Oksman, K.; Sain, M., Eds., American Chemical Society: Washington, DC, ACS Symp. Ser., **2006,** *938*, 221.
29. Horiike, S.; Matsuzawa, S. *J. Appl. Polym. Sci.* **1995,** *58*, 1335.
30. Roohani, M.; Habibi, Y.; Belgacem, N. M.; Ebrahim, G.; Karimi, A. N.; Dufresne, A. *Eur. Polym. J.* **2008,** *44*, 2489.

31. Arifuzzaman Khan, G. M.; Saheruzzaman, M.; Abdur Razzaque, S. M.; Sakinul Islam, M.; Shamsul Alam, M. *Indian J. Fibre Text. Res.* **2009,** *34*, 321.
32. Paralikar, S. A.; Simonsen, J.; Lombardi, J. *J. Membr. Sci.* **2008,** *320*, 248.
33. Chattopadhyay, H.; Sarkar, P. B. *Proc. Natl. Inst. Sci. India* **1946,** *12*, 23.
34. Cranston, E. D.; Gray, D. G. *Biomacromolecules* **2006,** *7*, 2522.
35. Kubo, S.; Kadla, J. F. *Biomacromolecules* **2003,** *4*, 561.
36. Peppas, N. A.; Merrill, E. W. *J. Appl. Polym. Sci.* **1976,** *20*, 1457.
37. Li, X.; Tabil, H. G.; Panigrahi, S. *J. Polym. Environ.* **2007,** *15*, 25.
38. Valadez-Gonzalez, A.; Cervantes-Uc, J. M.; Olayo, R.; Herrera-Franco, P. *J. Compos. Part B* **2005,** *36*, 597.
39. John, M. J.; Anandjiwala, R. D. *Polym. Compos.* **2008,** *29*, 187.
40. Fortunati, E.; Armentano, I.; Zhou, Q.; Iannoni, A.; Saino, E.; Visai, L.; Berglund, L. A.; Kenny, J. M. *Carbohydr. Polym.* **2012,** *87*, 1596.
41. Albano, C.; Gonzalez, J.; Ichazo, M.; Kaiser, D. *Polym. Degrad. Stabil.* **1999,** *66*, 179.
42. Ganan, P.; Garbizu, S.; Ponte, R. L.; Mondragon, I. *Polym. Compos.* **2005,** *26*, 121.
43. Lu, J.; Wang, T.; Drzal, L. T. *Compos.: Part A* **2008,** *39*, 738.
44. Abd El-Kader, K. M. *J. Appl. Polym. Sci.* **2003,** *88*, 589.
45. Qua, E. H.; Hornsby, P. R.; Sharma, H. S. S.; Lyons, G.; McCall, R. D. *J. Appl. Polym. Sci.* **2009,** *113*, 2238.
46. Frone, A. N.; Panaitescu, D. M.; Donescu, D.; Spataru, C. I.; Radovici, C.; Trusca, R.; Somoghi, R. *BioResources* **2011,** *6*, 487.
47. Li, W.; Yue, J.; Liu, S. *Ultrasonics Sonochem.* **2012,** *19*, 479.
48. Siqueira, G.; Bras, J.; Dufresne, A. *Polymers* **2010,** *2*, 728.
49. Colom, X.; Carrasco, F.; Pages, P.; Canavate, J. *Compos. Sci. Technol.* **2003,** *63*, 161.
50. Bondeson, D.; Oksman, K. *Compos. Interfaces* **2007,** *14*, 617.
51. Kamphunthong, W.; Hornsby, P.; Sirisinha, K. *J. Appl. Polym. Sci.* **2012,** *125*, 2, 1642.
52. Ibrahim, M. M.; El-Zawawy, W. K.; Nassar, M. A. *Carbohydr. Polym.* **2010,** *79*, 694.
53. Leppanen, K.; Andersson, S.; Torkkeli, M.; Knaapila, M.; Kotelnikova, N.; Serimaa, R. *Cellulose* **2009,** *16*, 999.
54. Elanthikkal, S.; Gopalakrishnapanicker, U.; Varghese, S.; Guthrie, J. T. *Carbohydr. Polym.* **2010,** *80*, 852.